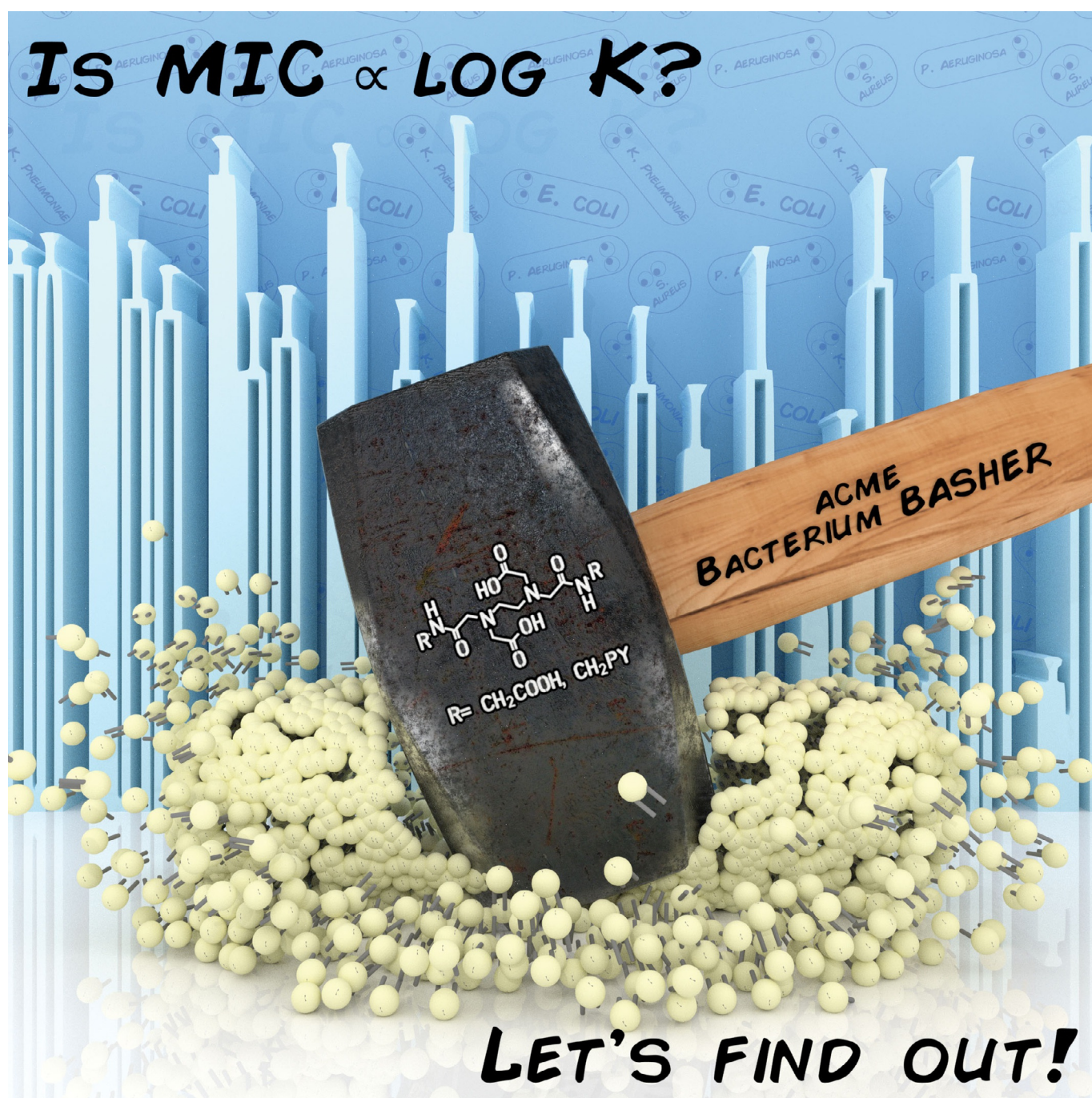■ Bioinorganic Chemistry |*Hot Paper*|

# On the Antibacterial Activity of Azacarboxylate Ligands: Lowered Metal Ion Affinities for Bis-amide Derivatives of EDTA do not mean Reduced Activity

Raminder S. Mulla,*[a] Marikka S. Beecroft,[b] Robert Pal,[a] Juan A. Aguilar,[a] Javier Pitarch-Jarque,[c] Enrique García-España,[c] Elena Lurie-Luke,[d] Gary J. Sharples,*[b] and J. A. Gareth Williams*[a]

**Abstract:** **EDTA** is widely used as an inhibitor of bacterial growth, affecting the uptake and control of metal ions by microorganisms. We describe the synthesis and characterisation of two symmetrical bis-amide derivatives of **EDTA**, featuring glycyl or pyridyl substituents: **AmGly₂** and **AmPy₂**. Metal ion affinities (log$K$) have been evaluated for a range of metals ($Mg^{2+}$, $Ca^{2+}$, $Fe^{3+}$, $Mn^{2+}$, $Zn^{2+}$), revealing less avid binding compared to **EDTA**. The solid-state structures of **AmGly₂** and of its $Mg^{2+}$ complex have been determined crystallographically. The latter shows an unusual 7-coordinate, capped octahedral $Mg^{2+}$ centre. The antibacterial activities of the two ligands and of **EDTA** have been evaluated against a range of health-relevant bacterial species, three Gram negative (*Escherichia coli*, *Pseudomonas aeruginosa*

and *Klebsiella pneumoniae*) and a Gram positive (*Staphylococcus aureus*). The **AmPy₂** ligand is the only one that displays a significant inhibitory effect against *K. pneumoniae*, but is less effective against the other organisms. **AmGly₂** exhibits a more powerful inhibitory effect against *E. coli* at lower concentrations than **EDTA** ($<3$ mM) or **AmPy₂**, but loses its efficacy at higher concentrations. The growth inhibition of **EDTA** and **AmGly₂** on mutant *E. coli* strains with defects in outer-membrane lipopolysaccharide (LPS) structures has been assessed to provide insight into the unexpected behaviour. Taken together, the results contradict the assumption of a simple link between metal ion affinity and antimicrobial efficacy.

## 1. Introduction

A number of strategies can be used to kill bacteria or restrict their growth, such as the use of oxidising solutions like bleach, elemental copper on surfaces, irradiation of materials with γ-rays and, more recently, exposure to nanoparticulate matter.[1–3] In addition to these 'inorganic' approaches, a battery of organic compounds can be applied, including disinfectants to disrupt bacterial cell envelopes, and antibiotics that target fundamental bacterial processes, often in a highly specific manner (e.g. blocking cell wall synthesis). Depriving bacteria of nutrients essential for growth, especially metal ions, can also prove effective,[4–7] since metal ions are critical for the proper function of many enzymes and play a role in resistance to oxidative stress.[8,9]

Metal ion starvation can be achieved by employing chelating ligands. Because of its ability to form stable complexes with a variety of metal ions, **EDTA** (Figure 1) is commonly incorporated in preservative formulations in many consumer products as diverse as mayonnaise and face creams.[10,11]

As part of a program to develop new chelating ligand systems that could be deployed in similar fashion to **EDTA**, we

surveyed the literature and found that, although a number of chelators have been investigated as potential antibacterial agents, their effect on biological systems was rarely rationalised in terms of their metal ion binding affinities.[12] Exceptions include two studies that treated the qualitative chelating ability of an aminocarboxylate ligand as a predictor of antibacterial activity, albeit without reference to specific metal ions.[13,14]

More recently, work on $Fe^{3+}$-sequestering agents demonstrated that ligands with greater $p(Fe^{3+})$ display lower minimum inhibitory concentration (MIC) values when a range of bacterial species were exposed to them {note that $p(M^{n+}) = -\log_{10}[M^{n+}]_{free}$, in which $[M^{n+}]$ is the concentration of "free" metal ion; high values are indicative of strong binding}.[15,16] It might be intuitive to expect that an increased metal ion affinity of a ligand would correlate with an increased level of metal ion depletion in a given bacterial growth environment, and consequently increase the likelihood of a detrimental effect on bacterial growth. In this study, we communicate our findings on two symmetrical bis-amide derivatives of **EDTA**, namely **AmGly₂** and **AmPy₂** (Figure 1), which contradict this attractive yet apparently overly simplistic interpretation, by showing that metal ion binding characteristics alone are not necessarily good predictors of the antibacterial effect of a given chelating ligand.

## 2. Results and Discussion

### 2.1. Synthetic strategies

Although structurally similar to one another, **AmGly₂** and **AmPy₂** were best prepared by different routes. We were able to access **AmGly₂** in gram-scale quantities by the nucleophilic ring opening of the symmetrical bis-anhydride of **EDTA** with glycine (Scheme 1) in a single step, without the need for protecting groups and in reasonable yields (ca. 40%). Occasionally, crystals of **AmGly₂** suitable for analysis by single crystal X-ray diffraction were isolable from synthetic runs (see Section 2.3).

This procedure can be considered a complement to that reported by Heathman,[17] in which the bis-anhydride of **EDTA** is

[a] Dr. R. S. Mulla, Dr. R. Pal, Dr. J. A. Aguilar, Prof. J. A. Gareth Williams
Department of Chemistry, Durham University
Durham, DH1 3LE (UK)
E-mail: raminder.mulla@durham.ac.uk
j.a.g.williams@durham.ac.uk

[b] M. S. Beecroft, Dr. G. J. Sharples
Department of Biosciences, Durham University
Durham, DH1 3LE (UK)
E-mail: gary.sharples@durham.ac.uk

[c] Dr. J. Pitarch-Jarque, Prof. E. García-España
Instituto de Ciencia Molecular, Universidad de Valencia
C/ Catedrático José Beltrán 2, 46980 Paterna, Valencia (Spain)

[d] Dr. E. Lurie-Luke
Procter and Gamble Technical Centres Limited, Rusham Park
Whitehall Lane, Egham, Surrey, TW20 9NW (UK)

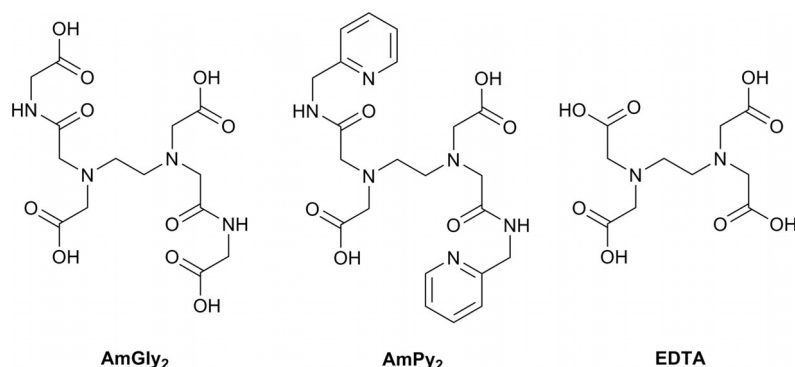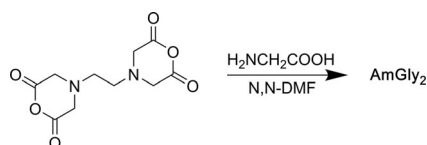Supporting information and the ORCID identification number(s) for the author(s) of this article can be found under https://doi.org/10.1002/chem.201800026.

**Figure 1.** The structures of the two ligands considered in this work, **AmGly$_2$** and **AmPy$_2$**, which are bis-amide derivatives of **EDTA**, whose structure is also shown for reference.



**Scheme 1.** Synthesis of **AmGly$_2$** from the bis-anhydride of **EDTA**.

ring-opened by the ethyl ester of glycine, followed by basic hydrolysis to afford **AmGly$_2$**. Higher overall yields of the product were reported compared to the one-pot approach described here, although the overall process is lengthier.

The same anhydride-based approach[18] was trialled for the synthesis of **AmPy$_2$**, but the strategy led to the formation of a crude mixture that was not amenable to conventional purification methods. A different approach was therefore adopted (Scheme 2), based on successive N-alkylation and protected intermediates that could easily be purified by column chromatography, similar to those pervasively used in the synthesis of chelating agents intended for lanthanide complexation.[19]

Preparation of intermediates **1**–**3** was straightforward using previously reported procedures. The structure of **1** in the solid state was determined by X-ray diffraction during the course of the work. Details are provided in the Supporting Information (Table S1). Alkylation of **2** with **3** gave amidoester **4**, which was purified via reverse phase column chromatography on a preparative scale prior to TFA-mediated *tert*-butyl ester deprotection in the presence of anisole as a cation scavenger, to afford

**AmPy$_2$** as its trifluoroacetate salt. The trifluoroacetate salt of **AmPy$_2$** was then passed down a column of DOWEX 1X8 anion exchange resin to remove any residual trifluoroacetate ion that could interfere with subsequent biological and pH-potentiometric studies of **AmPy$_2$**. The identities of **AmGly$_2$** and **AmPy$_2$** were confirmed by $^1$H and $^{13}$C NMR spectroscopy and electrospray mass spectrometry techniques, and sample purity evaluated by analytical HPLC. Combustion analysis gave satisfactory %CHN analytical data for **AmGly$_2$**, though the hygroscopic nature of **AmPy$_2$** led to results a little out of range.

## 2.2. Potentiometric measurements: protonation constants and metal affinities

Solutions for study were prepared containing 1 mM of the analyte ligand at an ionic strength of 0.15 M maintained using KCl. Four protonation constants were determined for both **AmGly$_2$** and **AmPy$_2$** with the first two protonations of each occurring at lower values than those of **EDTA** (Table 1). For all three ligands, the first protonation will take place on a tertiary amine group on the central ethylenediamine. The first protonation values are lower for **AmGly$_2$** and **AmPy$_2$** fragment due to the weakly electron-withdrawing effect that the amide groups exert on the neighbouring amines. Assignment of subsequent protonation events to either pyridines or carboxylates in **AmPy$_2$** on the basis of pH-potentiometry alone is not realistic due to the small differences in the protonation constants between each functional group.[62]
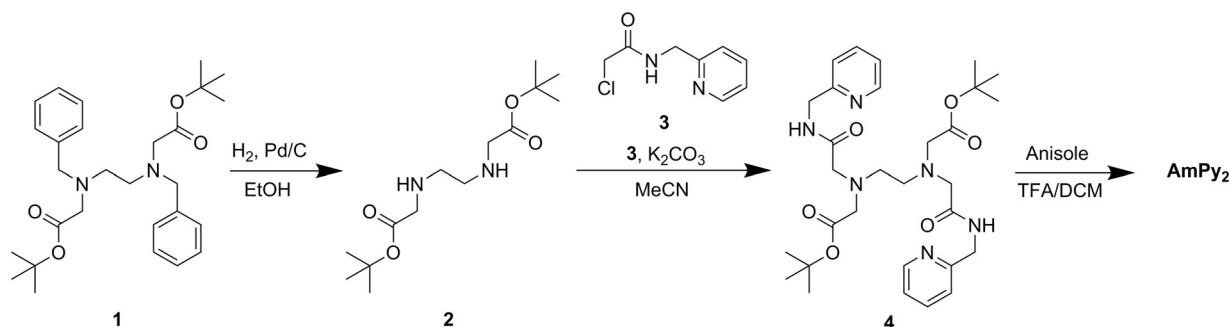


**Scheme 2.** Synthesis of **AmPy$_2$** using the benzyl protection route.

**Table 1.** Protonation constants at 25 °C, $I = 0.15$ M KCl, for **AmGly₂** and **AmPy₂**, with values for **EDTA** included for comparison. Charges are omitted for clarity. Data are the average of two independent experiments with the standard deviation in the last decimal place shown in parentheses. Previously published values for **AmGly₂** are included for comparison with the experimental data.

| Equilibrium[a] | logK(AmGly₂) exp. | lit.[b] | logK(AmPy₂) | logK(EDTA)[b] |
|---|---|---|---|---|
| L+H⇌HL | 7.22(2) | 7.34 | 7.34(2) | 10.17 |
| HL+H⇌H₂L | 4.17(2) | 4.35 | 5.10(2) | 6.11 |
| H₂L+H⇌H₃L | 3.54(3) | 3.63 | 4.22(2) | 2.68 |
| H₃L+H⇌H₄L | 3.38(3) | 2.96 | 2.96(2) | 2.0 |
| H₄L+H⇌H₅L | – | 1.81 | – | 1.5 |
| Log ß[d] | 18.30(3) | 20.09 | 19.62(3) | 22.46 |

[a] Charges omitted. [b] Values averaged from data reported by Martell[63] and Heathman[17] at $T = 25$ °C. [c] Data from Martell and Smith[64] at $T = 25$ °C and $I = 0.1$ M. [d] $\log \beta = \sum \log K$.

The protonation data were subsequently used to calculate metal ion-ligand association constants, as described in the Supporting Information. We selected five di/trivalent metal ions for study, being those commonly found in significant concentrations in biological systems (Ca²⁺, Mg²⁺, Fe³⁺, Mn²⁺ and Zn²⁺).[8] The resulting values are tabulated in Table 2.

What is immediately apparent from the data is the inferior binding of metal ions displayed by **AmGly₂** and **AmPy₂** in their fully deprotonated (L) forms compared to **EDTA**. Since the metal ions studied (Ca²⁺, Mg²⁺, Fe³⁺, Mn²⁺ and Zn²⁺) are all relatively hard, the loss of two charged, non-pendent carboxylate donor groups going from **EDTA** to **AmGly₂** and **AmPy₂** may in part be responsible for the reduction in chelate stabili-

ty. The order of complex stability, namely $Fe^{3+} > Zn^{2+} > Mn^{2+} > Ca^{2+} > Mg^{2+}$, is preserved in the case of the fully deprotonated forms of each ligand, meaning that changing the donor set from a tetracarboxylate to a biscarboxylate–bisamide configuration does not alter the selectivity of **AmGly₂** and **AmPy₂** for different metals compared to **EDTA** at high pH.

The more Lewis acidic metal ions studied ($Fe^{3+}$, $Mn^{2+}$ and $Zn^{2+}$) can either form hydroxo- complexes with **AmGly₂** and **AmPy₂**, or switch amide coordination mode from O- to N- coordination following deprotonation of the amide nitrogen atoms, as shown by the existence of MLH$_{-n}$ ($n = 1, 2, 3$) species in solution.[63] Speciation diagrams for **AmGly₂** are shown in Figure 2; corresponding diagrams for **AmPy₂** are provided in the Supporting Information (Figure S4).
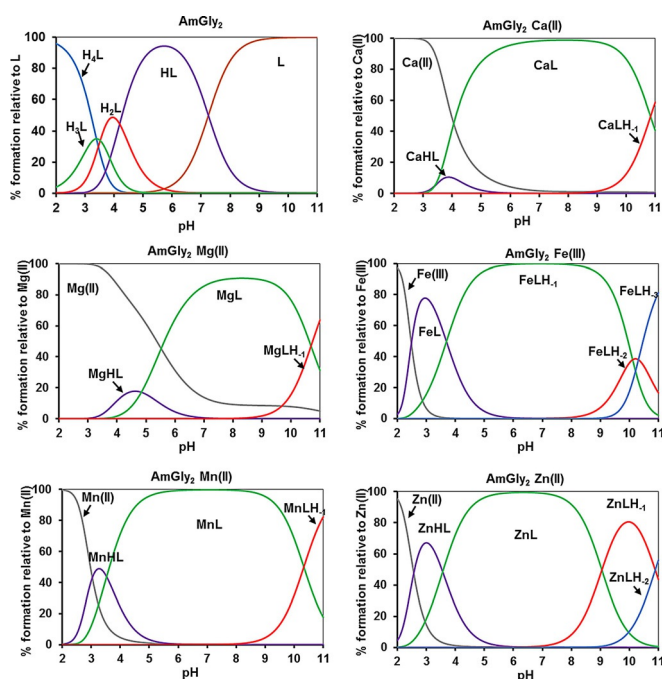


**Figure 2.** Distribution plots of the systems L:M (L = AmGly₂; M = H⁺, Ca²⁺, Mg²⁺, Fe³⁺, Mn²⁺, and Zn²⁺) in 1:1 molar ratio, [L] = [M] = 1×10⁻³ M (charges are omitted for clarity).

**Table 2.** Stepwise formation constants at 25 °C, $I = 0.15$ M KCl for metal ion complexes of **AmGly₂** and **AmPy₂**. Values are the average of two independent experiments. The values in parentheses are the standard deviation in the last significant Figure. Published values for **EDTA** are shown for comparison.

| Equilibrium[a] | Ca²⁺ | Mg²⁺ | Fe³⁺ | Mn²⁺ | Zn²⁺ |
|---|---|---|---|---|---|
| **AmGly₂[b]** | | | | | |
| ML+H⇌MHL | 3.34(5) | 4.78(6) | – | 3.53(2) | 3.58(2) |
| M+L⇌ML | 6.95(1) | 5.05(2) | 11.76(3) | 9.22(1) | 10.36(2) |
| ML⇌MLH₋₁+H | −10.84(3) | −10.68(4) | −3.69(2) | −10.32(2) | −9.07(2) |
| MLH₋₁⇌MLH₋₂+H | – | – | −10.11(2) | – | −10.88(3) |
| MLH₋₂⇌MLH₋₃+H | – | – | −10.30(7) | – | – |
| **AmPy₂[c]** | | | | | |
| MHL+H⇌MH₂L | | | | 3.81(2) | 3.75(4) |
| ML+H⇌MHL | – | – | 3.19(3) | 4.74(4) | 4.86(6) |
| M+L⇌ML | 6.56(3) | 3.38(9) | 12.76(2) | 8.64(4) | 10.4(1) |
| ML⇌MLH₋₁+H | – | −10.5(1) | −4.52(5) | −9.9(5) | −8.10(5) |
| MLH₋₁⇌MLH₋₂+2H | – | – | −9.55(8) | −10.34(6) | −10.1(2) |
| **EDTA[d]** | | | | | |
| M L+H⇌MHL | – | – | – | 3.10 | 3.00 |
| M+L⇌ML | 10.61 | 8.83 | 25.0 | 13.81 | 16.44 |

[a] Charges omitted. [b] Accompanying speciation diagrams for **AmGly₂** are given in Figure 2. [c] Speciation diagrams for **AmPy₂** are given in Supporting Information, Figure S4. [d] Data from Martell and Smith[64] at $T = 25$ °C and $I = 0.1$ M KCl.

From the studies performed, it seems unlikely that **AmGly₂** and **AmPy₂** form multinuclear species in which the donor groups appended to the amide linkage (i.e. -CH₂CO₂H for **AmGly₂** and -CH₂C₅H₄N for **AmPy₂**) participate in binding to the metal ions studied, since the fitting of the potentiometric data does not improve significantly when these systems are accounted for in the fitting models used. These groups may instead be used to interact with other cations present at higher concentrations than the metal ions investigated, which may in turn facilitate the formation of polymeric structures in the solid state, as discussed in Section 2.3.

A more useful expression of the metal ion affinity for these ligands can be found in quantities such as $p(M^{n+}) = -\log_{10}[M^{n+}]_{\text{free}}$[67], a measure of the free metal ion concentration in solution (analogous to pH) that can be calcu-

lated as described in the Supporting Information.[68] The measured factors in all of the relevant solution equilibria determined for **EDTA**, **AmGly$_2$** and **AmPy$_2$** at a given pH and the pM values thus calculated are shown in Table 3.

**Table 3.** $p[M^{n+}]$ values at pH 7.4 at 25 °C, $I = 0.15$ M KCl for **AmGly$_2$** and **AmPy$_2$**. [L] = 10 μmol dm$^{-3}$ and $[M^{n+}]$ = 1 μmol dm$^{-3}$.

| Species | AmGly$_2$ | AmPy$_2$ | EDTA |
|---|---|---|---|
| Ca$^{2+}$ | 7.7 | 7.3 | 8.8 |
| Mg$^{2+}$ | 6.2 | 6.0 | 7.0 |
| Fe$^{3+}$ | 16.2 | 16.3 | 23.2 |
| Mn$^{2+}$ | 9.9 | 9.3 | 12.0 |
| Zn$^{2+}$ | 11.1 | 11.1 | 14.6 |

Upon accounting for the multiple species in solution for each metal ion-ligand pair at pH 7.4 (a typical pH value for buffered liquid media such as Iso-sensitest), the trend in metal ion affinity is preserved with Fe$^{3+}$ being the metal ion most extensively sequestered and Mg$^{2+}$ the least. Moreover, when comparing the $p(M^{n+})$ values calculated for **AmGly$_2$** and **AmPy$_2$**, only small differences are noted. Most importantly, the $p(M^{n+})$ values at pH 7.4 clearly show that both **AmGly$_2$** and **AmPy$_2$** sequester all metal ions less extensively compared to **EDTA**, even when the multiple species present at pH 7.4 are taken into account. Both of these points will be returned to following discussion of the bacteriostatic action in Section 2.4.

## 2.3. Solid-state structures: AmGly$_2$ and its Mg$^{2+}$ complex

Single crystals suitable for X-ray diffraction analysis were obtained by the repeated recrystallization of metal-free **AmGly$_2$** in water. Slow evaporation of a solution prepared from a mixture of **AmGly$_2$** and Mg(NO$_3$)$_2$ at alkaline pH gave crystals of the magnesium complex **Mg(AmGly$_2$)NO$_3$**, which were also amenable to X-ray crystallography. Crystal data are summarised in Table S1 of the Supporting Information.

The structure of **AmGly$_2$** in the crystal reveals that the ligand is in its zwitterionic form (Figure 3). The carboxylate groups attached directly to the ethylenediamine unit (i.e. those containing oxygens O4 and O5 in the Figure) exist as their
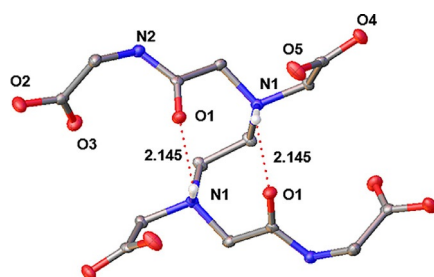
**Figure 3.** Molecular structure in the crystal of the AmGly$_2$ ligand, present as the zwitterionic form. Dashed line represents hydrogen bonds with their length in Å. Thermal ellipsoids are shown at the 50% probability level. For clarity, only crystallographically unique heteroatoms, or those involved in intramolecular hydrogen bonding interactions, are labelled.

anions, and the tertiary amines (N1) in each molecule are protonated. These protons on the tertiary amines participate in moderately strong intramolecular hydrogen bonding to the amide carbonyl oxygen atoms, $d$(H−O1) = 2.145 Å. In general, the measured bond lengths and angles do not greatly deviate from their expected ideal values.

The Mg$^{2+}$ complex **Mg(AmGly$_2$)NO$_3$** has a 1:1 stoichiometry with the central Mg$^{2+}$ ion adopting an unusual seven-coordinate geometry in a capped octahedral configuration (Figure 4, with key bond lengths and angles summarised in Table 4). The
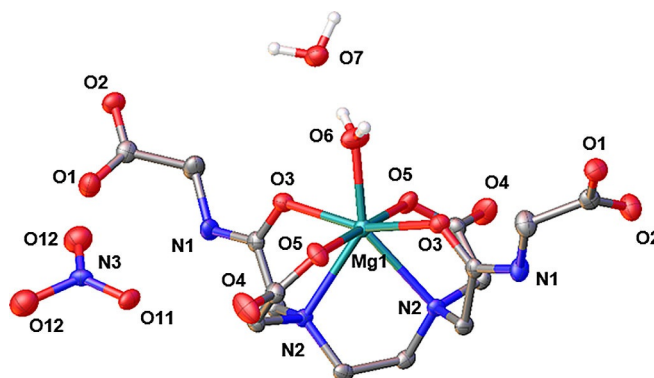
**Figure 4.** Molecular structure in the crystal of the **Mg(AmGly$_2$)** complex (Mg$^{2+}$ shown in turquoise). Thermal ellipsoids are shown at the 50% probability level. For clarity, the Na$^+$ ions coordinated to O2, O3, O4, O5, O11 and O12 and their associated water molecules are omitted, and only the heteroatoms are labelled.

**Table 4.** Selected bond lengths (Å) and angles (°) for **Mg(AmGly$_2$)**.

| Bond lengths | | Bond angles | |
|---|---|---|---|
| Bond | Length (Å) | Atoms | Angle (°) |
| Mg1−N2 | 2.421(3) | N2-Mg1-N2 | 73.86 (11) |
| Mg1−O3 | 2.2338 (19) | O5-Mg1-O3 | 100.66 (8) |
| Mg1−O5 | 2.087 (2) | O5-Mg1-N2 | 73.39 (8) |
| Mg1−O6 | 2.047 (3) | O6-Mg1-O3 | 81.26 (6) |

equivalent carboxylate oxygen atoms O5 are mutually *trans* to one another. Similarly the amide oxygen atoms are *trans* to one another, but in the equatorial plane. The ethylenediamine nitrogen atoms (N2) and a water molecule disordered across two sites bound to the central Mg$^{2+}$ via oxygen (O6) complete the coordination sphere. There is one nitrate ion per magnesium ion in the crystal; charge balance is presumably maintained by a proton whose location is undetermined.

The Mg$^{2+}$-to-donor bond lengths are fairly typical of other crystallographically characterised Mg$^{2+}$-aminocarboxylate complexes.[69–71] The amide oxygen−Mg$^{2+}$ bond lengths are seen to be longer than those of the carboxylate oxygen−Mg$^{2+}$ bonds, reflecting the reduced donor power of neutral amide oxygen groups for hard metal ions compared to anionic carboxylates. Interestingly, the H$_2$O−Mg$^{2+}$ length is shorter than both. In fact, a wide range of Mg$^{2+}$−O bond lengths has been observed in aminocarboxylate complexes of magnesium, attributed to

the size mismatch between these ligands and the Mg$^{2+}$ ion, which leads to the formation of distorted chelate rings and correspondingly elongated bonds.[69] Such distortions can be inferred in the structure of **Mg(AmGly$_2$)NO$_3$** from the marked deviation of the sum of the internal angles of each of the chelate rings from 540°.[70]

Although omitted from Figure 4 for clarity, oxygen atoms O2, O3, O4 and O5 also coordinate to hydrated Na$^+$ ions, a high concentration of which were available on account of the NaOH added to set the pH. The Na$^+$ ions attached to O3 and O5 also coordinate to the nitrate ion that is disordered across two sites. These Na$^+$—O interactions are the basis of an extended, wave-like polymeric structure, with each alternating **Mg(AmGly$_2$)** unit facing in opposite directions along the *b*-axis. In turn, these chains are linked by strong hydrogen bonds between the amide oxygen O2 on the **AmGly$_2$** ligand and the hydrogen on water molecules (O8) that are coordinated to Na$^+$ ions (Figure 5).

## 2.4. Bacterial growth inhibition studies

An optical-density based method was used to assess the growth of a selection of Gram negative and Gram positive bacteria in small-scale liquid culture (96-well plates), in the presence of varying concentrations of the chelating ligands. Studies were conducted in media of varying richness and salt concentration: Iso-sensitest (3 g/L NaCl) in the first instance, and in LB (Lysogeny Broth; 5 g/L NaCl) and low-salt LB (0.5 g/L NaCl) in certain cases. Iso-sensitest was chosen as the default media due to its being favoured by other workers for growth inhibition testing, including MIC determination,[20] along with having a more well-defined composition.

Bacteria grown to an optical density of 0.07 at $\lambda = 650$ nm were diluted 10-fold in fresh medium, equivalent to a 0.5 Mac-Farland standard,[20] and incubated with varying concentrations of **AmGly$_2$** or **AmPy$_2$** solutions; the latter were prepared in the same broth from a concentrated, aqueous, stock solution of either ligand. **EDTA** was tested in parallel to facilitate comparisons. To ensure the accuracy of stock ligand concentrations, we employed quantitative $^1$H NMR spectroscopy with the ROBUST5 pulse sequence for solvent suppression,[21] in the presence of an internal standard (t-butanol), to determine the precise concentrations of the **EDTA**, **AmGly$_2$** and **AmPy$_2$** stock solutions. Such an approach is preferable to relying on inferred stock concentrations from the mass of ligand dissolved in a given volume of water, owing to the hygroscopicity of the ligands.

To evaluate the spectrum of activity of **AmGly$_2$**, **AmPy$_2$** and **EDTA**, we selected four microorganisms for study—three Gram negatives (*Escherichia coli*, *Pseudomonas aeruginosa* and *Klebsiella pneumoniae*) and one Gram positive (*Staphylococcus aureus*). The K12 laboratory strain of *E. coli* was chosen as it lacks O-antigens that alter outer membrane architecture, and also because pathogenic variants of *E. coli* are important causative agents of gastrointestinal and urinary tract infections.[22] *P. aeruginosa* is a common cause of nosocomial infections, especially in burn victims and cystic fibrosis sufferers;[23, 24] it also differs from *E. coli* in the composition of its lipopolysaccharide (LPS) membrane.[25] *K. pneumoniae* is of interest because of its pathogenicity and antibiotic resistance;[26] furthermore, it has the capacity to produce a capsule that may serve to protect it from external stressors and is critically important in subverting the host immune response against it.[27] *S. aureus* was included as a Gram positive species with a different envelope structure and because of its capacity for pathogenicity, including highly drug-resistant forms.[28–30] Growth inhibition characteristics of **EDTA**, **AmGly$_2$** and **AmPy$_2$** on these four bacterial species are presented in Figure 6.

The data show that at ligand concentrations between 0.1 and 3.1 mm, **AmGly$_2$** is a more potent inhibitor of *E. coli* growth than **EDTA**, but appears to lose efficacy above 3.1 mm, leading to surprisingly unaffected *E. coli* growth at high [**AmGly$_2$**] relative to the control. The underlying causes of this biphasic response are discussed later in the text. In contrast, against *P. aeruginosa,* **AmGly$_2$** was less inhibitory than **EDTA** across all the tested concentrations. The reversal in relative sensitivities of the two species to **AmGly$_2$** and to **EDTA** in the low-to-mid concentration values used in this study may be associated with the fact that *P. aeruginosa* possesses O-antigens that are absent in the *E. coli* strain tested, whilst it also has more negatively charged phosphate groups clustered in the core oligosaccharide of its LPS layer. In contrast *E. coli* has fewer phosphate groups in a more dispersed arrangement.[31] It may be that these different charge configurations, and the
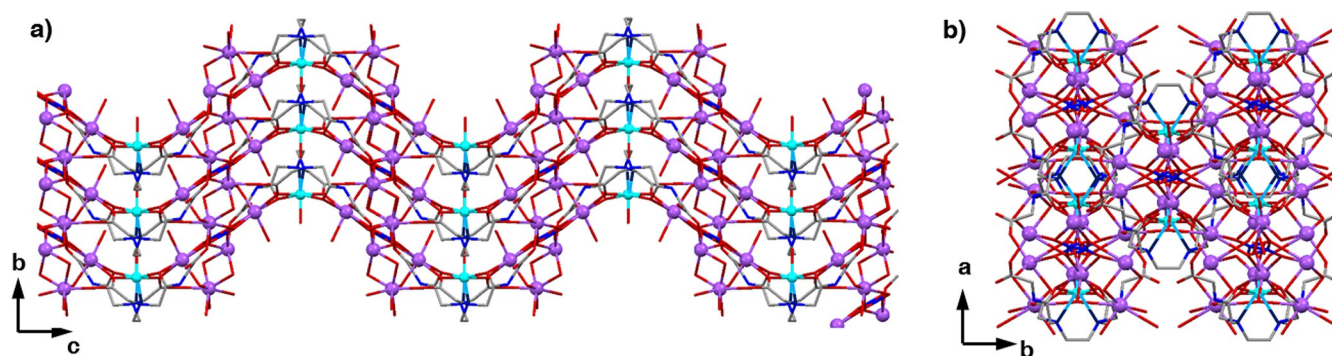


**Figure 5.** (a) Lateral and (b) end-on views of the polymeric structure of the Mg(AmGly$_2$)NO$_3$ complex. The hydrated Na$^+$ ions (purple) linking individual Mg(AmGly$_2$) units, as well as the coordinated Mg$^{2+}$ ions (turquoise), are shown as spheres for clarity.
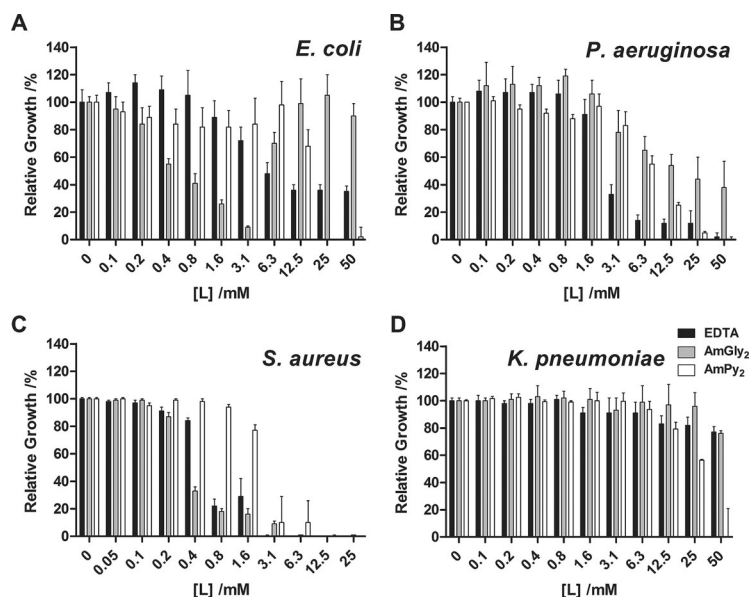
**Figure 6.** Effect of **EDTA**, **AmGly₂** and **AmPy₂** on the growth of (A) *E. coli*, (B) P. aeruginosa (C) S. aureus and (D) K. pneumoniae, in Iso-sensitest media. Data are the average of at least three replicates; error bars correspond to one standard deviation from the mean.

associated divalent cations used to stabilise the LPS layer, are affected very differently by **EDTA** compared to **AmGly₂**.

Remarkably, **AmPy₂**, when employed at high concentrations (>25 mM), displays greater inhibition than the other two ligands against all three Gram negative species. The inhibition of *K. pneumoniae* growth at high **AmPy₂** concentrations is especially interesting, since neither **EDTA** nor **AmGly₂** significantly inhibit its growth across the tested concentrations. The polysaccharide capsule secreted by *Klebsiella* species may provide a layer of protection from chelating ligands that directly target the outer membrane, similar to its capacity to resist antimicrobial peptides and copper.[32,33] Given the antibiotic resistance displayed by *K. pneumoniae*,[34] the use of ligands like **AmPy₂** may thus offer a useful strategy to control its growth.

Growth of the Gram positive *S. aureus* is inhibited at lower concentrations of **EDTA**, **AmGly₂** and **AmPy₂** than those required to inhibit the Gram negatives; indeed, no growth is observed at all for this organism at [**L**] >12.5 mM. **EDTA** and **AmGly₂** display very similar inhibitory behaviour against *S. aureus*, although **AmGly₂** starts to significantly inhibit growth at a lower concentration than **EDTA** (0.4 mM versus 0.8 mM respectively). **AmPy₂** on the other hand, does not significantly inhibit the growth of *S. aureus* below a concentration of 1.6 mM.

Gram positive bacteria lack an outer membrane, and so the detrimental effect of **EDTA, AmGly₂** and **AmPy₂** on *S. aureus* cannot be due to chelation-induced lipopolysaccharide (LPS) damage,[35–37] which can lead to leakage of cytoplasmic contents and cell death in the case of Gram negatives.[38,39] The sensitivity of *S. aureus* (which possesses only a single lipid bilayer) to **EDTA, AmGly₂** and **AmPy₂** clearly shows that chelation-induced growth inhibition is not restricted to bacteria with a Gram negative envelope architecture, in agreement with previous findings.[40–42]

As mentioned briefly, the dose responses of *P. aeruginosa*, *S. aureus* and *K. pneumoniae* are typical in that they are monophasic: beyond a critical ligand concentration, bacterial growth remains consistently low. However, the intriguing biphasic dose response of *E. coli* to **AmGly₂** is unusual and warranted further study. We initially surmised that this effect could be attributed to the aggregation of **AmGly₂** into a nonfunctional structure at higher concentrations. However, ES-MS and ¹H DOSY experiments on media containing **AmGly₂** that had been used to culture *E. coli* showed no evidence for such aggregation (see Supporting Information, Table S2).

## 2.5. Growth inhibition studies of *E. coli* mutants

We turned our attention to the outer membrane since it represents the first component of the Gram negative cell wall that would be contacted by a given chemical agent. The availability of a range of *E. coli* mutant strains exhibiting specific deficiencies in lipopolysaccharide (LPS) biosynthesis allowed us to investigate the potential contribution of the outer membrane in the biphasic dose response to **AmGly₂** (Figures 7 and Figure 8). Insertion-deletion mutants in the *hldD* (previous-
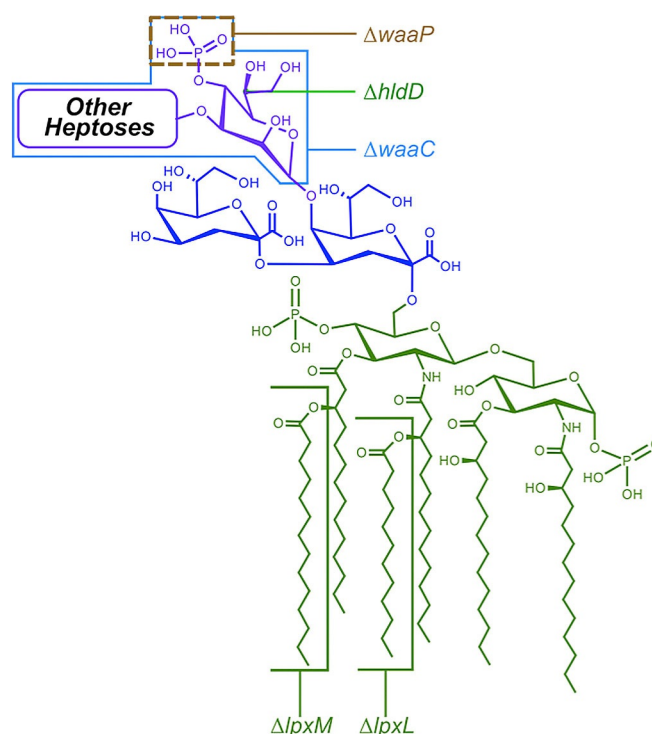


**Figure 7.** Structure of *E. coli* LPS, highlighting the lipid-A, Kdo₂ and HepI regions (shown in green, blue and purple, respectively). Structural features affected by deletion of the *lpxM*, *lpxL*, *waaC* or *waaP* genes are indicated (denoted Δ*lpxM*, Δ*lpxL*, Δ*waaC* and Δ*waaP*) and result in the highlighted portions being replaced by H atoms. The free hydroxyl groups resulting from mutation of *lpxM* or *lpxL* may be acylated by other fatty acids.[44] Deletion of the *hldD* (Δ*hldD*) gene precludes an inversion of configuration at the highlighted stereocentre on HepI, leading to the mutant structure bearing the opposite epimer to the one shown.
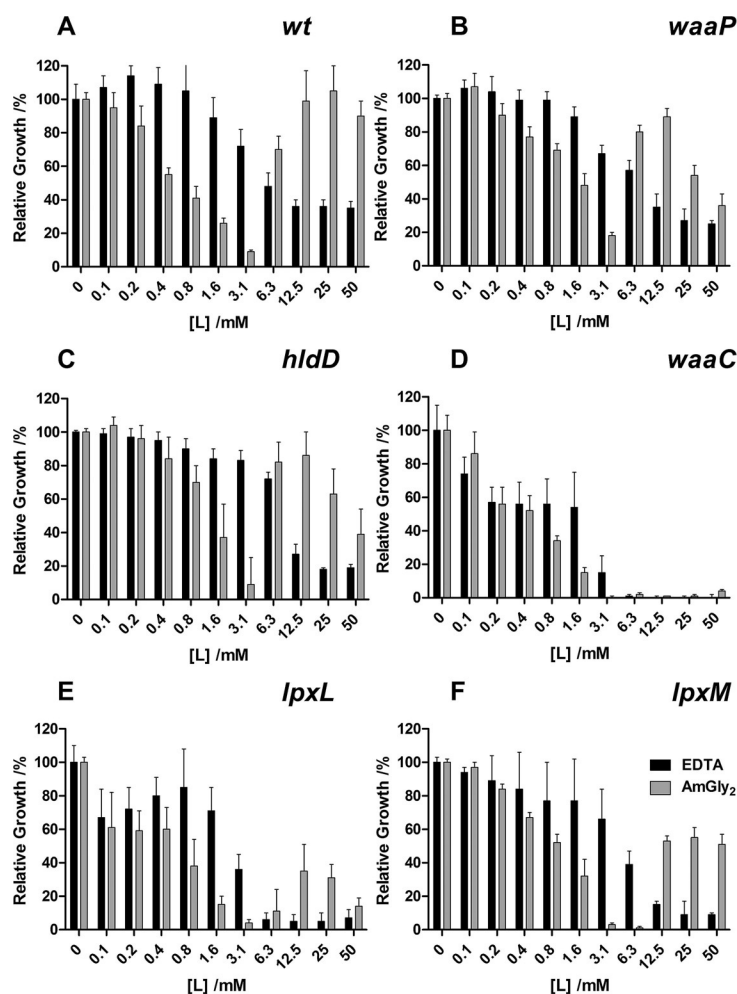
**A** *wt*
**B** *waaP*
**C** *hldD*
**D** waaC
**E** *lpxL*
**F** *lpxM*

■ EDTA
■ AmGly₂

**Figure 8.** Effect of **EDTA** and **AmGly₂** on the growth of the *E. coli* (A) wild-type, (B) *waaP*, (C) *hldD*, (D) waaC, (E) *lpxL* and (F) *lpxM* mutants of EDTA and **AmGly₂** in Iso-sensitest media (see Figure 7 for illustration of the LPS sites affected in the mutants). Data for the isogenic *E. coli* wild-type are reproduced here from Figure 5 to aid comparison with the mutant strains. Results are the average of three independent experiments, all performed in technical triplicate; error bars correspond to one standard deviation from the mean.

ly known as *rfaD*), *lpxL*, *lpxM*, *waaC* and *waaP* genes were obtained from the Keio collection.[43] Differences in the structure of the LPS layer between these mutants are highlighted through the colour-coded diagram in Figure 7 and summarised in the caption. The sensitivity of these mutants to **AmGly₂** and **EDTA** was assessed in the same way as the wild type studies in Figure 6, discussed above.

Starting from the basal components of the LPS structure (shown in green in the structure in Figure 7), it is apparent that the *lpxL* and *lpxM* mutants are more sensitive to **EDTA** and **AmGly₂** than the wild type (Figure 8 E–F). Although it has been shown that free hydroxyl groups in lipid A that arise due to *lpxL* and *lpxM* deletion may be acylated instead by *lpxX* (X = L, M or P, depending on the gene that remains in the mutant in question) to maintain the cell permeability barrier,[44] it has been noted that the *E. coli lpxM* mutant is more permeable to certain antibiotics than the wild-type,[45] and that *lpxL lpxM* double mutants display enhanced membrane permeability,

suggesting that the full complement of acyltransferases are needed to maintain *E. coli* outer membrane integrity.[46] The results suggest that hydrophobic components of lipid A are an important factor in protecting *E. coli* against chelating agents. However, a biphasic response is still evident in the susceptibility of these strains to **AmGly₂** (Figure 4 E–F).

Mutants with differing core oligosaccharide structures (blue units in Figure 7) were next examined. The Kdo₂ transferase gene *waaA* (*kdtA*) is essential for *E. coli* growth and so this part of the oligosaccharide structure cannot be studied.[43] We investigated mutations that would lead to changes in the LPS oligosaccharide structure distal to the Kdo₂ motif. For example, the *hldD* mutant has been shown, as with *lpxM*, to lead to increased membrane permeability to certain drugs.[47,48] From Figure 8, it can be seen that epimerisation of HepI due to *hldD* mutation leads to only a minor increase in sensitivity to **EDTA** and **AmGly₂** at higher concentrations, [**L**] > 12.5 mM, relative to the wild type.

The *waaP* gene encodes a kinase that phosphorylates HepI,[49] and deletion of *waaP* increases susceptibility to hydrophobic drugs.[50,51] This is most likely due to a loss of the stabilising effect on the LPS layer of the interaction between phosphate groups with $Mg^{2+}$ and $Ca^{2+}$.[52] Surprisingly, the *waaP* mutant displays a similar inhibition profile to the wild type when exposed to **EDTA**, which suggests that phosphorylation of HepI—and the coordinative interactions in which phosphorylated HepI participates—are not particularly important for growth in the presence of **EDTA**. The *waaP* mutant is however slightly more sensitive to **AmGly₂** at concentrations > 3.1 mM (as with *hldD*), suggesting that the recovery of *E. coli* growth at high concentrations of **AmGly₂** has some dependence on the HepI component of LPS. Yet, both *waaP* and *hldD* mutants retain a biphasic dose response to **AmGly₂** (Figure 8 B and C).

The importance of components distal to Kdo₂ in the recovery of *E. coli* growth at high concentrations of **AmGly₂** was probed using a *waaC* mutant.[51,53–55] The protein encoded by *waaC* is responsible for the transfer of HepI to the Kdo₂ fragment of LPS.[56] HepI is in turn phosphorylated by *waaP* and serves as the point from which other heptoses (and ultimately the O-antigen in most pathogenic strains) are attached, meaning that the absence of *waaC,* and therefore HepI, leads to a highly truncated LPS structure in mutant cells.[57–59] When the *waaC* mutant is exposed to **AmGly₂**, no biphasic growth response is observed: instead, a dose response similar to that of **EDTA** is apparent, and little or no recovery of growth occurs at higher **AmGly₂** concentrations (Figure 8 D).

We investigated whether loss of the biphasic response to **AmGly₂** was due to an osmotic effect on membrane permeability, by stressing cells in a low ionic strength LB medium (LS-LB). When *waaC* mutants are exposed to **EDTA** and **AmGly₂** in

LS-LB media, the biphasic dose response is restored, although the growth recovery remains considerably less pronounced than that seen for the wild type in Iso-sensitest (Figure 9). This observation suggests that the restoration of growth with the *E. coli* wild type at high **AmGly₂** concentrations in Iso-sensitest medium may have an osmotic component to the mechanism, in addition to involving HepI and structures distal to it. Viability assays were used to confirm that the *waaC* mutant is not grossly affected by the reduced salt content of LS-LB in comparison to normal LB media (Supporting Information, Figure S3).
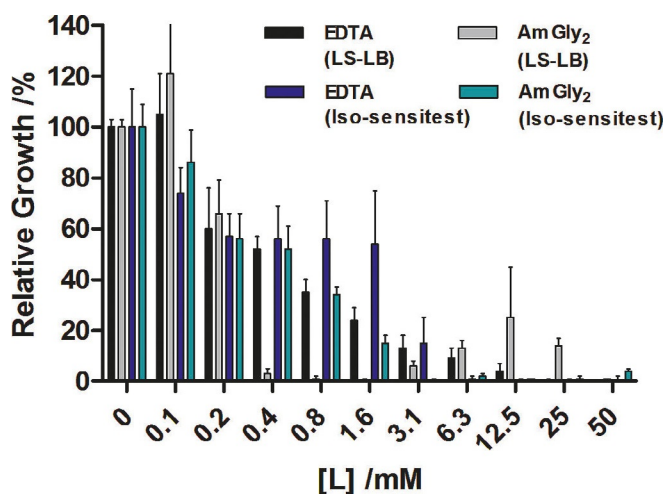


**Figure 10.** Effect of **EDTA** and **AmGly₂** on the growth of the *E. coli* (A) phoQ and (B) phoP mutants in Iso-sensitest media. Data are the average of three independent experiments, all performed in technical triplicate; error bars correspond to one standard deviation from the mean.



**Figure 9.** Comparison of the growth of the *E. coli* waaC mutant at increasing concentrations of **EDTA** or **AmGly₂** in LS-LB and Iso-sensitest media. The data for **EDTA** and **AmGly₂** on waaC in Iso-sensitest from Figure 3 D are reproduced here to facilitate comparisons. Data are the average of three independent experiments, each performed in technical triplicate; error bars represent one standard deviation from the mean.

In investigating the importance of the outer membrane in the biphasic dose response, the role of the pleiotropic *phoQ–phoP* system was also examined.[60] PhoQ is a membrane protein that senses changes in $Mg^{2+}$ concentrations and, if $[Mg^{2+}]$ is sufficiently low, phosphorylates the transcription factor PhoP, which in turn functions as a transcriptional activator of the *pagP* and the *pbgPE* operons among others. Increased expression of *pagP* and *pbgPE* leads to LPS modification via the palmitoylation of Lipid A and incorporation of 4-aminoarabinose into its structure,[60] changes which are thought to contribute to resistance to cationic antimicrobial agents due to a decrease in membrane permeability. Mutants lacking either of these genes therefore lack the ability to effect a reduction in membrane permeability in response to reduced $[Mg^{2+}]$, a condition which could be brought about by chelation of $Mg^{2+}$ by either **EDTA** or **AmGly₂**.

Data for the *phoQ* and *phoP* mutants are shown in Figure 10. It can be seen that their growth is completely inhibited at $[EDTA] > 12.5$ mM, unlike the wild type, suggesting that these genes (or genes activated by them) are involved in the
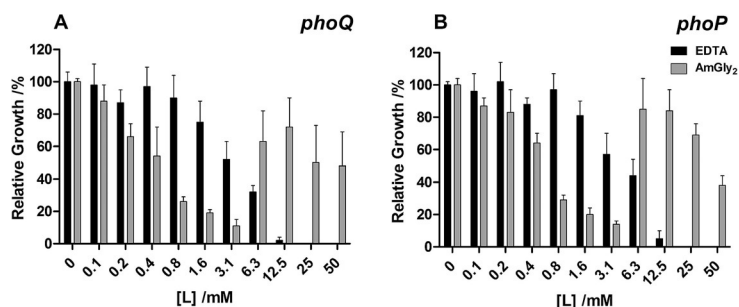
*E. coli* wild type defence mechanism against chelating ligands that reduce the extracellular $[Mg^{2+}]$. This is not the case for **AmGly₂**, to which the *phoQ* and *phoP* mutants both show a biphasic dose response similar to that observed with the wild-type (compare Figs. 10 and 6A), with the most severe inhibition once again observed at $[AmGly_2] = 3.1$ mM, followed by substantially improved growth at higher concentrations. These observations suggest that exposure to **AmGly₂** does not lead to activation of *phoQ* and *phoP* in the wild type as a defence mechanism, whereas with **EDTA** it does.

There is a slight reduction in growth of *phoQ* and *phoP* at the highest **AmGly₂** concentrations, similar to that observed with the *waaP* and *hldD* mutants (Figure 6 B and C). Since a biphasic dose response to **AmGly₂** was observed for the *E. coli* wild type and all of the mutants except for *waaC*, one might postulate that **AmGly₂** may act as a membrane permeabiliser in a similar way to **EDTA**, but may be less able to reduce extracellular metal ion concentrations. This may result in a greater flux of metal ions across damaged cell membranes when bacteria are grown in the presence of the **AmGly₂**, leading to increased growth past a critical point, before which, cell membranes are damaged, but selectivity in ion uptake is not lost and so growth is limited by the reduced metal ion flux. The *waaC* mutant could exhibit monophasic behaviour in Iso-sensitest, despite the increased permeability to metal ions, due to the severity of its LPS truncation, leading to more facile cell lysis.

## 2.6. Fluorescence microscopy of *E. coli* exposed to EDTA or AmGly₂

To further investigate the differing effects of **EDTA** and **AmGly₂** on *E. coli*, fluorescent dyes were employed to monitor the integrity of cells exposed to these two ligands. Concentrations of **EDTA** and **AmGly₂** that resulted in 15 and 50% growth reductions were selected and wild-type *E. coli* cells analysed using the SYTO™ 9 dye that distinguishes living cells with an intact outer membrane from those which have lost membrane integrity resulting in entry of a second added dye, namely propidium iodide. Live cells (those with an intact membrane) and dead cells (those with a disrupted membrane) were visualized
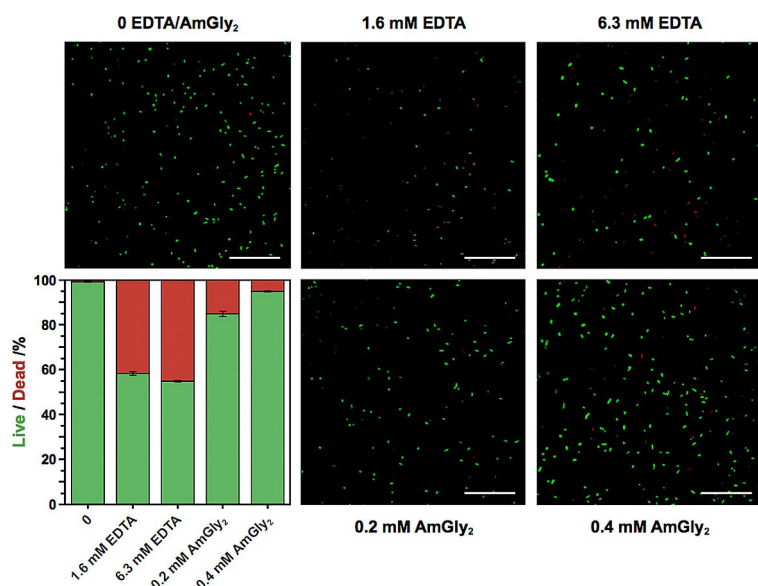
**Figure 11.** Effect of **EDTA** and **AmGly$_2$** on the viability of *E. coli* wild-type cells. The proportion of cells stained with SYTO™ **9** (live, green) and propidium iodide (dead, red) was determined by fluorescence microscopy. Data are the average of five independent experiments with >3000 cells counted from 25 fields of view. Error bars correspond to one standard deviation from the mean. Representative images of each of the fields of view in the presence or absence of **EDTA** or **AmGly$_2$** are also shown. The scale bar is 50 µm in all cases.

and counted and the results are shown in Figure 11. The observations can be summarised as follows:

Examination of an untreated control (i.e. no ligand added) revealed that only a very small fraction (1.3%) of the cells present had lost membrane integrity.

Exposure to 1.6 mм **EDTA** (corresponding to a 15% reduction in growth relative to the untreated control) resulted in 42% dead cells present in the sample being analysed. At [**EDTA**] = 6.25 mм (50% growth inhibition), an average of 45% of the cells present in the sample stained as dead, which is only a small increase in the fraction of dead cells given the drastic change in growth inhibition.

Exposure to 0.2 mм **AmGly$_2$** (15% growth inhibition) resulted in an average of 14% of the cells in the culture staining as dead. When [**AmGly$_2$**] was increased to 0.4 mм, the proportion of "dead" cells decreased to 5%.

These observations suggest that the inhibitory actions of **EDTA** and **AmGly$_2$** on *E. coli* growth differ in their origins. The growth reduction observed with **EDTA** correlates with loss of membrane integrity and suggests that **EDTA**, at least in part, reduces bacterial growth by killing a proportion of the cells in a way that **AmGly$_2$** does not.

The data may suggest that **EDTA** and its metal complexes interact with the *E. coli* outer membrane to a greater extent than **AmGly$_2$** and its metal complexes. Speciation calculations based on the potentiometric titration data for **EDTA**, **AmGly$_2$** (Table 2) and their selected metal ion complexes (M$^{n+}$ = Ca$^{2+}$, Mg$^{2+}$, Fe$^{3+}$, Mn$^{2+}$ and Zn$^{2+}$) show that, at pH 7.4, **AmGly$_2$** and M$^{n+}$–**AmGly$_2$** complexes are more negatively charged than those of **EDTA** (Supplementary information, Table S3). Given the high negative charge density of *E. coli* LPS due to its phos-

phate groups (Figure 6), we suggest that the reduced membrane permeabilisation observed when *E. coli* is treated with **AmGly$_2$** compared to **EDTA** may be due to the greater coulombic repulsion between LPS and **AmGly$_2$**/ M$^{n+}$–**AmGly$_2$**. The significant charge differences in LPS structure between *E. coli* and *P. aeruginosa*[31] may then go some way to explain why **AmGly$_2$** fails to show a biphasic response with the latter organism (Figure 6A).

These charge differences may mean that **AmGly$_2$** is also restricted to depleting metals from the medium to starve cells and reduce growth. The biphasic response observed for *E. coli* could fit with a cellular response to tolerate metal starvation. In contrast, **EDTA** may target bacterial membrane integrity directly in addition to removing essential metals from the growth medium.

## 3. Concluding Remarks

Two symmetrical bis-amide derivatives of **EDTA**, **AmGly$_2$** and **AmPy$_2$**, have been prepared via novel routes and their activities in inhibiting bacterial growth have been evaluated and compared with that of **EDTA**, which is widely used as a bacteriostatic agent. The solid state structures of metal free **AmGly$_2$** and its Mg$^{2+}$ complex **Mg(AmGly$_2$)NO$_3$** have also been determined, with the latter adopting an extended polymeric structure not unlike previous **EDTA** amides studied.[72]

The **AmPy$_2$** ligand—although less effective at lower concentrations against *E. coli*, *P. aeruginosa* and *S. aureus* than **EDTA** and **AmGly$_2$**—is the only ligand of the set that displays a significant inhibitory effect against *K. pneumoniae,* albeit requiring concentrations ≥ 25 mм.

The **AmGly$_2$** ligand exhibits a more powerful inhibitory effect against *E. coli* at lower concentrations than **EDTA** (≤ 3.1 mм) or **AmPy$_2$**, but loses its efficacy at higher concentrations. Studies on the effect of **AmGly$_2$** and **EDTA** on a number of mutant *E. coli* strains producing defective LPS structures to investigate the biphasic dose response showed that only severe truncations in LPS led to a conventional, monophasic dose response, as demonstrated by the action of **AmGly$_2$** against the *waaC* mutant.

The biphasic dose response of *E. coli* to **AmGly$_2$** is thought to have an osmotic component, as evidenced by its partial restoration in the *waaC* mutant in low-salt media. More generally, work on the Mg$^{2+}$-dependent *phoQ* and *phoP* systems showed that they are involved in the defence mechanism of *E. coli* against **EDTA** but not **AmGly$_2$**, as shown by the similarity of the *phoQ* and *phoP* mutant dose response to that of the wild-type, when exposed to **AmGly$_2$**.

Remarkably, studies into the metal ion affinities of **AmGly$_2$** and **AmPy$_2$** show that the metal ion affinities to Ca$^{2+}$, Mg$^{2+}$, Fe$^{3+}$, Mn$^{2+}$ and Zn$^{2+}$ are lower than those of **EDTA**, even when the impact of the ligand ionisation state on metal ion affinities is accounted for. This contradicts previous understanding on the efficacy of chelating antimicrobials: there is no

simple link between metal ion affinity and antimicrobial efficacy. It is clear that interactions between the outer membrane of an organism as well as metal ion affinity ought to be considered when rationalising efficacy.

Altogether, these data provide evidence that metal ion affinity is not the primary determinant of bacterial growth inhibition for this class of molecules and that **EDTA** bis-amides warrant further investigation as a new class of chelating antimicrobials, potentially offering activity against more resistant species.

## Acknowledgements

## Conflict of interest

The authors declare no conflict of interest.

[1] I. Sondi, B. Salopek-Sondi, *J. Colloid Interface Sci.* **2004**, *275*, 177–182.
[2] J. S. Kim, E. Kuk, K. N. Yu, J.-H. Kim, S. J. Park, H. J. Lee, S. H. Kim, Y. K. Park, Y. H. Park, C.-Y. Hwang, *Nanomed. Nanotechnol. Biol. Med.* **2007**, *3*, 95–101.
[3] J. R. Swathy, M. U. Sankar, A. Chaudhary, S. Aigal, Anshup, T. Pradeep, *Sci. Rep.* **2014**, *4*, 7161.
[4] B. D. Corbin, E. H. Seeley, A. Raab, J. Feldmann, M. R. Miller, V. J. Torres, K. L. Anderson, B. M. Dattilo, P. M. Dunman, R. Gerads, *Science* **2008**, *319*, 962–965.
[5] S. M. Damo, T. E. Kehl-Fie, N. Sugitani, M. E. Holt, S. Rathi, W. J. Murphy, Y. Zhang, C. Betz, L. Hench, G. Fritz, *Proc. Natl. Acad. Sci. USA* **2013**, *110*, 3841–3846.
[6] K. W. Becker, E. P. Skaar, *FEMS Microbiol. Rev.* **2014**, *38*, 1235–1249.
[7] T. G. Nakashige, B. Zhang, C. Krebs, E. M. Nolan, *Nat. Chem. Biol.* **2015**, *11*, 765–771.
[8] K. J. Waldron, J. C. Rutherford, D. Ford, N. J. Robinson, *Nature* **2009**, *460*, 823–830.
[9] J. A. Imlay, *Nat. Rev. Microbiol.* **2013**, *11*, 443–454.
[10] J. R. Hart, *J. Chem. Educ.* **1984**, *61*, 1060.
[11] J. R. Hart, *J. Chem. Educ.* **1985**, *62*, 75.
[12] T. Bergan, J. Klaveness, A. J. Aasen, *Chemotherapy* **2001**, *47*, 10–14.
[13] H. Haque, A. D. Russell, *Antimicrob. Agents Chemother.* **1974**, *5*, 447–452.
[14] H. Haque, A. D. Russell, *Antimicrob. Agents Chemother.* **1974**, *6*, 200–206.
[15] Y.-Y. Xie, M.-S. Liu, P.-P. Hu, X.-L. Kong, D.-H. Qiu, J.-L. Xu, R. C. Hider, T. Zhou, *Med. Chem. Res.* **2013**, *22*, 2351–2359.
[16] M.-X. Zhang, C.-F. Zhu, Y.-J. Zhou, X.-L. Kong, R. C. Hider, T. Zhou, *Chem. Biol. Drug Des.* **2014**, *84*, 659–668.
[17] C. R. Heathman, T. S. Grimes, P. R. Zalupski, *Inorg. Chem.* **2016**, *55*, 2977–2985.
[18] Z. Zhu, X. Wang, T. Li, S. Aime, P. J. Sadler, Z. Guo, *Angew. Chem. Int. Ed.* **2014**, *53*, 13225–13228; *Angew. Chem.* **2014**, *126*, 13441–13444.
[19] L. Lattuada, A. Barge, G. Cravotto, G. B. Giovenzana, L. Tei, *Chem. Soc. Rev.* **2011**, *40*, 3019.
[20] J. M. Andrews, *J. Antimicrob. Chemother.* **2001**, *48*, 5–16.
[21] J. A. Aguilar, S. J. Kenwright, *Analyst* **2016**, *141*, 236–242.
[22] J. B. Kaper, J. P. Nataro, H. L. T. Mobley, *Nat. Rev. Microbiol.* **2004**, *2*, 123–140.
[23] B. H. Iglewski, in *Med. Microbiol.* (Ed.: S. Baron), University Of Texas Medical Branch At Galveston, Galveston (TX), **1996**.
[24] J. S. Lam, V. L. Taylor, S. T. Islam, Y. Hao, D. Kocíncová, *Front. Microbiol.* **2011**, *2*, https://doi.org/10.3389/fmicb.2011.00118.
[25] A. H. Fensom, G. W. Gray, *Biochem. J.* **1969**, *114*, 185–196.
[26] C. A. Broberg, M. Palacios, V. L. Miller, *F1000prime Rep.* **2014**, *6*, 64.
[27] M. S. Lawlor, J. Hsu, P. D. Rick, V. L. Miller, *Mol. Microbiol.* **2005**, *58*, 1054–1073.
[28] B. S. Cooper, G. F. Medley, S. P. Stone, C. C. Kibbler, B. D. Cookson, J. A. Roberts, G. Duckworth, R. Lai, S. Ebrahim, *Proc. Natl. Acad. Sci. USA* **2004**, *101*, 10223–10228.
[29] T. J. Foster, *Nat. Rev. Microbiol.* **2005**, *3*, 948–958.
[30] H. F. Chambers, F. R. DeLeo, *Nat. Rev. Microbiol.* **2009**, *7*, 629–641.
[31] H. Nikaido, *Microbiol. Mol. Biol. Rev.* **2003**, *67*, 593–656.
[32] G. Bitton, V. Freihofer, *Microb. Ecol.* **1977**, *4*, 119–125.
[33] E. Llobet, J. M. Tomás, J. A. Bengoechea, *Microbiology* **2008**, *154*, 3877–3886.
[34] J. D. D. Pitout, P. Nordmann, L. Poirel, *Antimicrob. Agents Chemother.* **2015**, *59*, 5873–5884.
[35] J. G. Voss, *J. Gen. Microbiol.* **1967**, *48*, 391–400.
[36] L. Leive, *Biochem. Biophys. Res. Commun.* **1965**, *21*, 290–296.
[37] M. Vaara, *Microbiol. Rev.* **1992**, *56*, 395–411.
[38] K. Matsushita, O. Adachi, E. Shinagawa, M. Ameyama, *J. Biochem.* **1978**, *83*, 171–181.
[39] N. A. Amro, L. P. Kotra, K. Wadu-Mesthrige, A. Bulychev, S. Mobashery, G. Liu, *Langmuir* **2000**, *16*, 2789–2796.
[40] N. D. Hammer, E. P. Skaar, *Curr. Opin. Microbiol.* **2012**, *15*, 10–14.
[41] J. M. Kraniak, L. A. Shelef, *J. Food Sci.* **1988**, *53*, 910–913.
[42] B. R. D. Short, M. A. Vargas, J. C. Thomas, S. O'Hanlon, M. C. Enright, *J. Antimicrob. Chemother.* **2006**, *57*, 104–109.
[43] T. Baba, T. Ara, M. Hasegawa, Y. Takai, Y. Okumura, M. Baba, K. A. Datsenko, M. Tomita, B. L. Wanner, H. Mori, *Mol. Syst. Biol.* **2006**, *2*, 1–11.
[44] B. Schilling, J. Hunt, B. W. Gibson, M. A. Apicella, *Innate Immun.* **2014**, *20*, 269–282.
[45] H. Xu, J. Ling, Q. Gao, H. He, X. Mu, Z. Yan, S. Gao, X. Liu, *Vet. Microbiol.* **2013**, *166*, 516–526.
[46] M. K. Vorachek-Warren, S. Ramirez, R. J. Cotter, C. R. H. Raetz, *J. Biol. Chem.* **2002**, *277*, 14194–14205.
[47] W. G. Coleman, *J. Biol. Chem.* **1983**, *258*, 1985–1990.
[48] L. Ding, B. L. Seto, S. A. Ahmed, W. G. Coleman, *J. Biol. Chem.* **1994**, *269*, 24384–24390.
[49] J. A. Yethon, D. E. Heinrichs, M. A. Monteiro, M. B. Perry, C. Whitfield, *J. Biol. Chem.* **1998**, *273*, 26310–26316.
[50] J. A. Yethon, C. Whitfield, *J. Biol. Chem.* **2001**, *276*, 5498–5504.
[51] Z. Wang, J. Wang, G. Ren, Y. Li, X. Wang, *Mar. Drugs* **2015**, *13*, 3325–3339.
[52] S. Gronow, H. Brade, *J. Endotoxin Res.* **2001**, *7*, 3–23.
[53] C. R. H. Raetz, C. Whitfield, *Annu. Rev. Biochem.* **2002**, *71*, 635–700.
[54] M. E. Bauer, R. A. Welch, *Infect. Immun.* **1997**, *65*, 2218–2224.
[55] B. Kneidinger, C. Marolda, M. Graninger, A. Zamyatina, F. McArthur, P. Kosma, M. A. Valvano, P. Messner, *J. Bacteriol.* **2002**, *184*, 363–369.
[56] S. Grizot, M. Salem, V. Vongsouthi, L. Durand, F. Moreau, H. Dohi, S. Vincent, S. Escaich, A. Ducruix, *J. Mol. Biol.* **2006**, *363*, 383–394.
[57] L. Chen, W. G. Coleman, *J. Bacteriol.* **1993**, *175*, 2534–2540.
[58] J. L. Kadrmas, C. R. Raetz, *J. Biol. Chem.* **1998**, *273*, 2799–2807.
[59] D. E. Heinrichs, J. A. Yethon, C. Whitfield, *Mol. Microbiol.* **1998**, *30*, 221–232.
[60] E. A. Groisman, *J. Bacteriol.* **2001**, *183*, 1835–1842.
[61] L. D. Pettit, *Chem. Int.- Newsmag. IUPAC* **2009**, *28*, 14–15.
[62] P. Caravan, S. J. Rettig, C. Orvig, *Inorg. Chem.* **1997**, *36*, 1306–1315.
[63] R. J. Motekaitis, A. E. Martell, *J. Am. Chem. Soc.* **1970**, *92*, 4223–4230.
[64] R. M. Smith, A. E. Martell, *Critical Stability Constants*, Springer US: Imprint: Springer, Boston, MA, **1989**.
[65] R. A. Bulman, N. Jobanputra, R. Kuroda, A. McKinnon, P. J. Sadler, *Inorg. Chem.* **1987**, *26*, 2483–2486.
[66] A. E. O. Fisher, D. P. Naughton, *J. Struct. Chem.* **2006**, *47*, 87–90.
[67] W. R. Harris, K. N. Raymond, F. L. Weitl, *J. Am. Chem. Soc.* **1981**, *103*, 2667–2675.
[68] L. Alderighi, P. Gans, A. Ienco, D. Peters, A. Sabatini, A. Vacca, *Coord. Chem. Rev.* **1999**, *184*, 311–318.

[69] J. J. Stezowski, R. Countryman, J. L. Hoard, *Inorg. Chem.* **1973**, *12*, 1749–1754.

[70] E. Passer, J. G. White, K. L. Cheng, *Inorg. Chim. Acta* **1977**, *24*, 13–23.

[71] N. Nakasuka, M. Shiro, *Acta Crystallogr. Sect. C* **1989**, *45*, 1487–1490.

[72] R. S. Mulla, J. Pitarch-Jarque, E. García-España, T. Desa, E. Lurie-Luke, J. A. G. Williams, *ChemistrySelect* **2017**, *2*, 5045–5050.